ELSEVIER

Journal of Nuclear Materials 289 (2001) 329–333

journal of nuclear materials

www.elsevier.nl/locate/jnucmat

Thermophysical properties of zirconium hydride and uranium–zirconium hydride

B. Tsuchiya [a,*], J. Huang [a], K. Konashi [a], M. Teshigawara [b], M. Yamawaki [c]

[a] *The Oarai Branch, Institute for Materials Research, Tohoku University, Oarai-machi, Ibaraki-ken 311-1313, Japan*
[b] *Spallation Neutron Laboratory, Tokai Research Establishment, Japan Atomic Energy Research Institute, Tokai-mura, Ibaraki-ken 319-1195, Japan*
[c] *Department of Quantum Engineering and Systems Science, Graduate School of Engineering, University of Tokyo, 7-3-1 Hongo, Bunkyo-ku, Tokyo 113-8656, Japan*

Received 7 June 2000; accepted 30 November 2000

Abstract

Thermal diffusivities of ε-phase Zirconium hydrides ($ZrH_{1.69-2.00}$) were measured in the temperature range from 300 to 600 K by means of a laser-flash method. The thermal diffusivity of ε-phase Zr hydrides increased with increasing hydrogen concentration and decreased with increasing temperature. The thermal diffusivities of ε-phase ZrH_x with $x > 1.83$ were larger than that of α-phase Zr. The experimental data on the thermal diffusivity were expressed with the equations as a function of temperature and composition. Moreover, the thermal conductivities of ε-phase Zr hydrides were estimated from the measured data of the thermal diffusivity and the reported data of the density and specific heat. It was found that the ε-phase Zr hydrides were better thermal conductors than α-phase Zr and δ-phase Zr hydrides. The thermal diffusivity and conductivity of U–ZrH_x were also estimated with the ones of ZrH_x and U. © 2001 Elsevier Science B.V. All rights reserved.

PACS: 65.90.+i; 67.80.Gd; 72.15.Eb

1. Introduction

Hydride fuels have been used in research reactors (e.g., TRIGA reactors) for many years [1,2]. Recently, the transmutation method of nuclear wastes using actinide hydrides has been proposed [3]. It was pointed out that one of the important research and development items for establishment of the transmutation method is to develop stable actinide hydride fuels under reactor irradiation conditions. Specifically, thermal conductivity data of actinide hydride fuels are necessary for the design of the hydride fuel pin.

The actinide hydride fuels consist of actinide metal phases and actinide hydride phases. The Zr hydride phase is also included in the target and plays an important role for controlling the hydrogen decomposition pressure. The thermal diffusivity of ZrH_x was measured using a laser-flash method and was expressed with the equations as a function of temperature and composition in the present work. The thermal conductivity was calculated from the relation of the measured thermal diffusivity, the literature data of the density and specific heat. Finally, the thermal conductivity of U–ZrH_x ($1.6 \leqslant x \leqslant 2.0$) which had not been published yet in the TRIGA reports [1,2], except for U–$ZrH_{1.6}$, was estimated with the reported values of metal uranium.

2. Experiments

2.1. Hydrogenation

Specimens of ZrH_x ($x = 1.69$–2.00) were prepared by hydrogenation of zirconium in a Sieverts apparatus. The

---

[*] Corresponding author. Fax: +81-29 267 4947.
E-mail address: tsuchiya@imr.tohoku.ac.jp (B. Tsuchiya).

PII: S0022-3115(01)00420-2

pure Zr metal, 99.8 wt% in purity and 1.0 mm in thickness and 6.3 or 10.0 mm in diameter, was placed in a quartz vessel. It was then evacuated and kept in vacuum under a pressure of 4.0×10^{-5} Pa. Before the hydrogenation, a little residual hydrogen in Zr was removed out by flush heating in vacuum to 1073 K for 1 h (t_h in Fig. 1). In the present study, Zr hydride specimens with various compositions were prepared by controlling hydrogen pressures. For example, Fig. 1 shows the hydrogen absorption history of $ZrH_{1.83}$, where Zr metal was hydrogenated at a pressure of 1.0×10^5 Pa and a temperature of 1053 K for 2 h (t_s) and cooled down to room temperature at the rate of 8.7×10^{-3} K/s. The pressure rapidly decreased when hydrogen gas was induced into the quartz vessel by opening the valve (t_o). With the decrease of temperature, hydrogen was gradually absorbed in Zr (t_c). No microcracks were detected by the scanning electron microscope (SEM) technique, in spite of the lattice expansion due to hydrogen absorption. Although the concentration of hydrogen retained in Zr was measured both from the hydrogen pressure changes and mass gains after hydrogenation, unfortunately, weight of the specimens used was too limited to obtain accurately the fraction of hydrogen to Zr (H/Zr). The X-ray diffraction (XRD) technique was used to evaluate the composition as well as the phase. The compositions of the hydride specimens were determined based on the experimental data by Cantrell et al. [4]. Fig. 2 shows the selected part of the XRD patterns of δ-phase $ZrH_{1.66}$ and ε-phase $ZrH_{1.69–2.00}$ specimens. It is noticed that the diffraction peak of (2 2 0) of ε-phase shifts to a lower angle side with the increase of hydrogen concentration, while that of (0 2 2) goes to the opposite direction. This implies the expansion of the axis *a* and the contraction of axis *c* in the face-centered tetragonal (fct) structure.

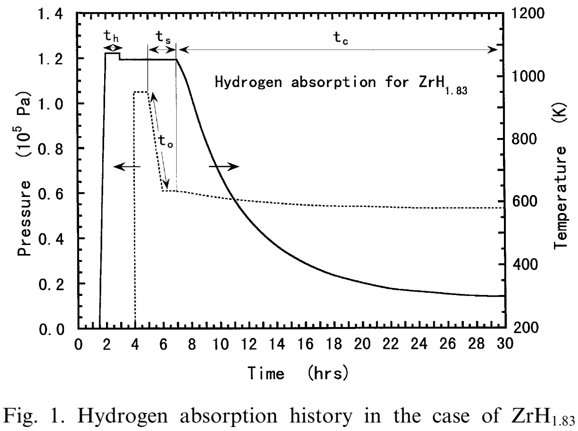

Fig. 1. Hydrogen absorption history in the case of $ZrH_{1.83}$ specimen. The hydrogenation is performed using Sieverts apparatus.

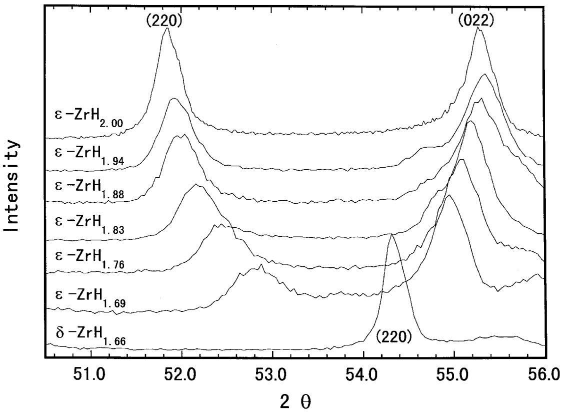

Fig. 2. X-ray diffraction patterns of δ-phase $ZrH_{1.66}$ and ε-phase $ZrH_{1.69–2.00}$.

2.2. Thermal diffusivity measurements

The thermal diffusivity measurement was made for the ε-phase $ZrH_{1.69–2.00}$ in the temperature range from 300 to 600 K using the laser-flash method. Details of the laser-flash method can be found in the references [5,6]. The specimen was measured up to around 600 K, because Zr hydride tends to decompose at high temperatures [2,7]. Reproduction ability of the measurement was good for both increasing and decreasing temperature processes, which indicated that little hydrogen was released in the measurement. The phase-transition from ε to δ has also been reported to take place at a high temperature [2]. In the present work, a high-temperature XRD detection showed that no phase-transition occurred up to 600 K.

3. Experimental results and discussion

3.1. Thermal diffusivity and thermal conductivity of ZrH_x

The experimental results of the thermal diffusivity measurements at room temperature are shown as a function of the composition for δ- and ε-phase Zr hydrides. It can be seen in Fig. 3 that the present results agree well with the data of $ZrH_{1.70}$ and $ZrH_{1.81}$ (△) reported by Weeks et al. [6]. It should be noted that the thermal diffusivities of ε-phase (●) increase with increasing hydrogen concentration and are larger than that for α-phase Zr (◇) [8] especially when $x > 1.83$. On the other hand, the thermal diffusivities of the δ-phase are almost constant, independent of the hydrogen concentration. Their hydrogen concentration dependence of thermal diffusivity was similar to that of electrical resistivity [9]. These results indicate that Zr hydrides have a metallic nature and electronic heat conduction is the

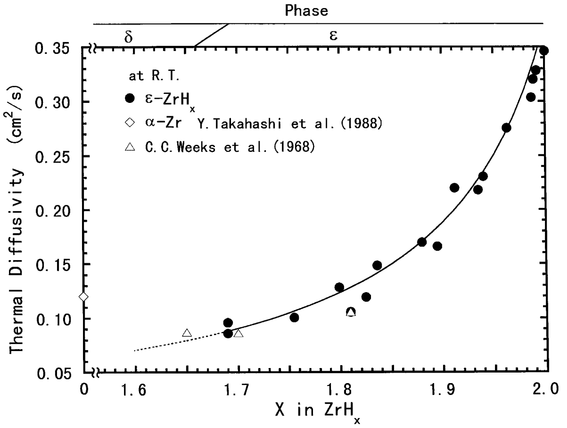

Fig. 3. Thermal diffusivity versus composition for δ- and ε-phase Zr hydrides at room temperature. (●) represents the experimental values for ε-phase ZrH_x ($x = 1.69–2.00$). (△) and (◇) represent the experimental values for δ- and ε-phase ZrH_x ($x = 1.65–1.81$) [6] and α-phase Zr [8], respectively.

dominant process. The curve in Fig. 3 can be expressed as a function of compositions of ZrH_x ($1.6 \leqslant x \leqslant 2.0$) as described latter.

Fig. 4 shows the temperature dependence of the experimental thermal diffusivities for ε-$ZrH_{1.76}$, ε-$ZrH_{1.83}$, ε-$ZrH_{1.90}$ and ε-$ZrH_{1.94}$ in the temperature range from 300 to 600 K. As shown in Fig. 4, the data measured during temperature increasing (●, ◆, ▲, ▼) are in good accord with those during temperature decreasing (○, ◇, △, ▽). It indicates that neither oxidation on the specimen surface nor the release of hydrogen occurs during the measurement. It is also seen in Fig. 4 that the thermal diffusivities with various compositions decrease with increasing temperature, as the result for $ZrH_{1.81}$ has been reported by Weeks et al. [6].

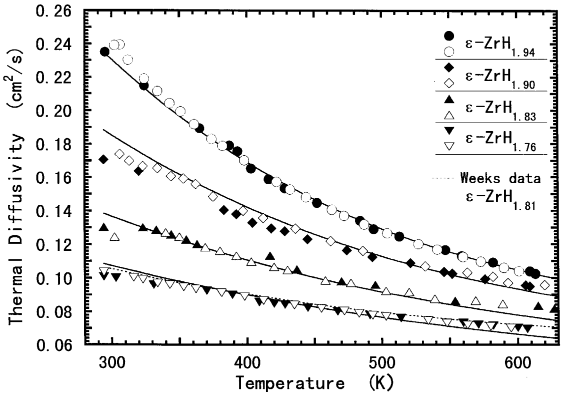

Fig. 4. Temperature dependence of thermal diffusivities for ε-$ZrH_{1.76}$, ε-$ZrH_{1.83}$, ε-$ZrH_{1.90}$ and ε-$ZrH_{1.94}$. The dashed curve represents the thermal diffusivity of ε-$ZrH_{1.81}$ measured by Weeks et al. [6]. The solid curves are expressed with Eq. (1) obtained by fitting the experimental data.

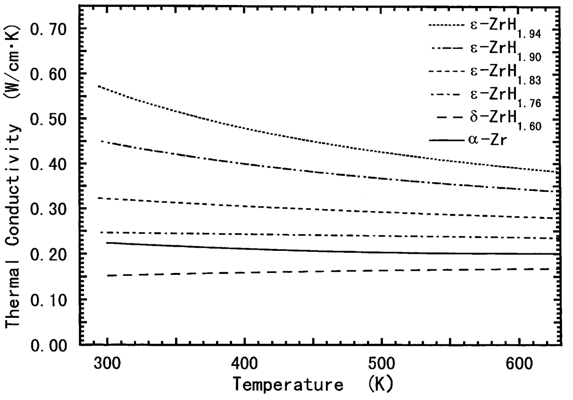

Fig. 5. Temperature dependence of thermal conductivities for δ-$ZrH_{1.60}$, ε-$ZrH_{1.76}$, ε-$ZrH_{1.83}$, ε-$ZrH_{1.90}$ and ε-$ZrH_{1.94}$, which were calculated from the relation of $\lambda = \alpha C_p \rho$, as compared with that for α-Zr [8].

The temperature dependence of thermal diffusivities α (cm²/s) for several compositions x ($1.6 \leqslant x \leqslant 2.0$) can be expressed by the following equation:

$$\alpha = \frac{67.9}{\{T + 1.62 \times 10^3 (2.00 - x) - 1.18 \times 10^2\}} - 1.16 \times 10^{-2}, \qquad (1)$$

where T (K) represents the temperature.

The thermal conductivities for δ-$ZrH_{1.60}$, ε-$ZrH_{1.76}$, ε-$ZrH_{1.83}$, ε-$ZrH_{1.90}$ and ε-$ZrH_{1.94}$ were calculated from the relation of $\lambda = \alpha C_p \rho$, where λ, C_p and ρ represented the thermal conductivity, the specific heat and the density, respectively, as shown in Fig. 5. The values of C_p and ρ for δ-Zr hydrides have been described with the temperature and composition in the Simnad report [2]. The effect of density change due to thermal expansion was not taken into account in the calculation, where for example the decrease in the density at 600 K is less than 1.0% [6]. It is seen in Fig. 5 that the temperature dependence of the thermal diffusivity greatly contributes to that of the thermal conductivity. Moreover, the ε-ZrH_x is a better thermal conductor than that of α-Zr [8] and δ-$ZrH_{1.60}$ at temperatures up to 600 K.

3.2. Thermal diffusivity and thermal conductivity of U–ZrH_x

45 wt% U–$ZrH_{1.60}$ was prepared by means of the Sieverts apparatus. It was observed from XRD and SEM analyses that the α-phase U of 1.0 μm in grain size was uniformly dispersed in the bulk of δ-phase $ZrH_{1.60}$. The results are similar to those observed by Simnad et al. [1]. It is assumed that the thermal diffusivity α_{U-ZrH_x}

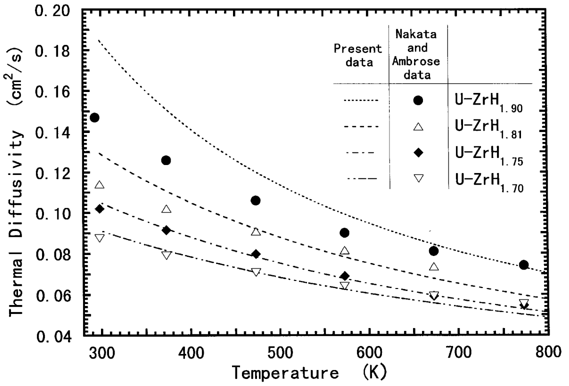

Fig. 6. Comparison for the calculated values with the experimental ones of thermal diffusivities for 10 wt% U–$ZrH_{1.70}$, –$ZrH_{1.75}$, –$ZrH_{1.81}$ and –$ZrH_{1.90}$ [11,12].

of U–ZrH_x for the two-phase component material can be expressed by the simple rule of mixture (ROM) [10]:

$$\alpha_{\mathrm{U-ZrH}_x} = V_{\mathrm{U}}\alpha_{\mathrm{U}} + V_{\mathrm{ZrH}_x}\alpha_{\mathrm{ZrH}_x}, \tag{2}$$

where α_i and V_i are the thermal diffusivity and the volume fraction of the constituent phase i. Fig. 6 shows the $\alpha_{\mathrm{U-ZrH}_x}$ of 10 wt% U–ZrH_x ($x = 1.70$, 1.75, 1.81 and 1.90). The curves in Fig. 6 are represented based on Eq. (2) with the $\alpha_{\mathrm{ZrH}x}$ of ZrH_x ($x = 1.70$, 1.75, 1.81 and 1.90) which are obtained with Eq. (1) and the α_{U} (0.11–0.12 cm^2/s in the temperature range 300–800 K) of U [8] and $V_{\mathrm{ZrH}_x} = 96.8\%$ and $V_{\mathrm{U}} = 3.2\%$.

Moreover, it is also assumed that the thermal conductivity $\lambda_{\mathrm{U-ZrH}_x}$ of U–ZrH_x for the two-phase component material can be expressed by ROM [10]:

$$\lambda_{\mathrm{U-ZrH}_x} = V_{\mathrm{U}}\lambda_{\mathrm{U}} + V_{\mathrm{ZrH}_x}\lambda_{\mathrm{ZrH}_x}, \tag{3}$$

where λ_i is the thermal conductivity of the constituent phase i. The thermal conductivities $\lambda_{\mathrm{U-ZrH}_x}$ of 45 wt% U–ZrH_x ($x = 1.60$, 1.76, 1.83, 1.90 and 1.94) were estimated in the temperature range 300–800 K from the λ_{ZrH_x} of ZrH_x ($x = 1.60$, 1.76, 1.83, 1.90 and 1.94) in Fig. 5 and the λ_{U} of U [8] and $V_{\mathrm{ZrH}_x} = 80.5\%$ and $V_{\mathrm{U}} = 19.5\%$, as shown in Fig. 7. The estimated values of thermal conductivity for 45 wt% U–$ZrH_{1.60}$ (dashed curve) were close to the thermal conductivity of 0.18 W/(cm K) (solid curve) used for the design calculation of the TRIGA reactor [2].

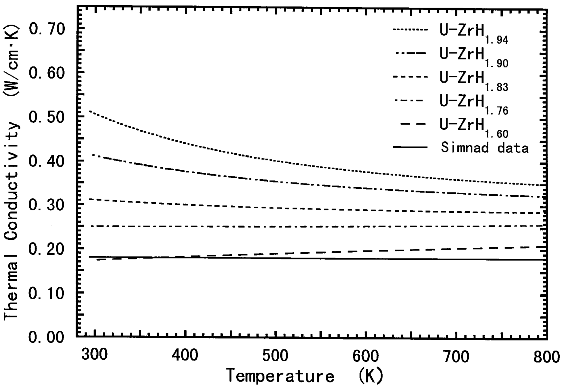

Fig. 7. Temperature dependence of thermal conductivities for 45 wt% U–$ZrH_{1.60}$, –$ZrH_{1.76}$, –$ZrH_{1.83}$, –$ZrH_{1.90}$ and –$ZrH_{1.94}$ which were estimated from those of $ZrH_{1.60–1.94}$ and U. The solid line represents the thermal conductivity which has been published in the TRIGA reports [2].

4. Summary

The temperature dependence of the thermal diffusivities of ε-$ZrH_{1.69–2.00}$ has been studied at temperatures 300–600 K by means of the laser-flash method. The thermal diffusivities of ε-ZrH_x at room temperature increased with the increase of hydrogen concentration. The values of ε-ZrH_x with $x > 1.83$ are larger than that of α-Zr. The thermal diffusivities with various compositions decrease as the temperature increases. The following equation of the thermal diffusivity of $ZrH_x(1.6 \leqslant x \leqslant 2.0)$ in the temperature range $300 \leqslant T \leqslant 600$ K was obtained by fitting the experimental data.

$$\alpha = \frac{67.9}{\{T + 1.62\times10^3(2.00-x) - 1.18\times10^2\}} - 1.16 \times 10^{-2}.$$

Moreover, the thermal conductivities were calculated with the equation of the thermal diffusivity and the references of the density and specific heat. The ε-Zr hydrides are better thermal conductors than α-phase Zr metal and δ-phase Zr hydrides in the temperature range 300–600 K.

The thermal diffusivity and conductivity of U–ZrH_x were estimated with those of ZrH_x and U. The thermal conductivity of 45 wt% U–$ZrH_{1.60}$ was 0.17–0.20 W/(cm K) in the temperature range 300–800 K and was close to the reported data of the TRIGA reactor.

References

[1] M.T. Simnad et al., Nucl. Technol. 28 (1976) 31.
[2] M.T. Simnad, Nucl. Eng. Des. 64 (1981) 403.
[3] T. Sanda, K. Fujimura, K. Kawashima. M. Yamawaki, K. Konashi, in: Proceedings of the Global '97, International Conference of the Future Nuclear System, Yokohama, Japan, 5–10 October 1997, p. 326.
[4] J.S. Cantrell, R.C. Bowman Jr., D.B. Sullenger, J. Phys. Chem. 88 (1984) 918.
[5] W.J. Parker, R.J. Jenkins, C.P. Butler, G.L. Abbott, J. Appl. Phys. 32 (1961) 1679.

[6] C.C. Weeks, M.M. Nakata, C.A. Smith, in: Proceedings of the Seventh Conference on Thermal Conductivity, 13–16 November 1967, 1968, p. 387.
[7] J.A. Llauger, G.N. Walton, J. Nucl. Mater. 97 (1981) 185.
[8] Y. Takahashi, M. Yamawaki, K. Yamamoto, J. Nucl. Mater. 154 (1988) 141.
[9] P.W. Bickel, T.G. Berlincourt, Phys. Rev. B 2 (1970) 4807.
[10] J. Kováčik, Scripta Mater. 39 (1998) 153.
[11] M.M. Nakata, C.J. Ambrose, R.A. Finch, in: Proceedings of the Sixth Conference on Thermal Conductivity, 19–21 October 1966, p. 479.
[12] C.J. Ambrose, R.E. Taylor, R.A. Finch, in: Proceedings of the Fourth Conference on Thermal Conductivity, 13–16 October 1964.